

# Microbial Electrochemical Energy Storage and Recovery in a Combined Electrotrophic and Electrogenic Biofilm

Matthew D. Yates,<sup>\*,†,‡</sup> Li Ma,<sup>‡</sup> Joshua Sack,<sup>§,||</sup> Joel P. Golden,<sup>†</sup> Sarah M. Strycharz-Glaven,<sup>†</sup> Scott R. Yates,<sup>‡</sup> and Leonard M. Tender<sup>†</sup>

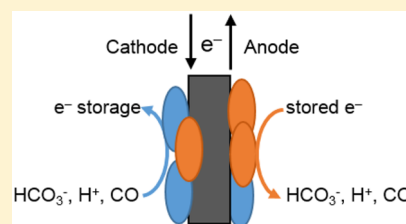
<sup>†</sup>Center for Bio/Molecular Science and Engineering, Naval Research Laboratory, Washington, D.C. 20375, United States

<sup>‡</sup>U.S. Salinity Laboratory, U.S. Department of Agriculture Agricultural Research Service, Riverside, California 92507, United States

<sup>§</sup>Center for Bio/Molecular Science and Engineering, Naval Research Laboratory, Washington, D.C. 20375, United States

## S Supporting Information

**ABSTRACT:** Here we report enrichment from a marine-derived inoculum of a nonphotosynthetic electroactive biofilm that is capable of both consuming electricity (electrotrophy) and producing electricity (electrogenesis) from a single electrode. With the alternation of the electrode potential between  $-0.4$  and  $0.0$   $V_{SHE}$  every 10 min, alternating anodic and cathodic currents increased in lock step (maximum current density of  $\pm 1.4 \pm 0.4$   $A/m^2$  in both modes, Coulombic efficiency of  $\sim 98\%$  per charge–discharge cycle), which is consistent with alternating between generation and consumption of energy storage compounds by the biofilm. Cyclic voltammetry exhibited a single sigmoid-shaped feature spanning anodic and cathodic limiting currents centered at  $-0.15$   $V_{SHE}$ , a phenomenon not observed to date for an electroactive biofilm, and square wave voltammetry exhibited reversible peaks at  $-0.15$  and  $-0.05$   $V_{SHE}$ , suggesting the same redox cofactor(s) facilitates electron transport at the biofilm–electrode interface in both modes. Hydrogen and carbon monoxide, known energy and/or carbon sources for cellular metabolism, but no volatile fatty acids, were detected in reactors. Cells and cell clusters were spread across the electrode surface, as seen by confocal microscopy. These results suggest that a single microbial electrochemical biofilm can alternate between storing energy and generating power, furthering the potential applicability of bioelectrochemical systems.



## INTRODUCTION

Bioelectrochemical systems (BESs) are a biotechnological platform developed around utilizing microorganisms as electrode catalysts. BESs hold promise as an alternative strategy for energy generation and storage because, unlike conventional (abiotic) catalysts, microbes self-assemble using abundant resources for maintenance and growth (organic carbon,  $CO_2$ , water, etc.), self-regenerate, thrive under a wide range of conditions, and can potentially be altered genetically to catalyze specified reactions that abiotic catalysts cannot.

Biofilms harboring electroactive microorganisms on the electrodes of BESs are able to catalyze a variety of processes governed by their environment, the electrochemical potential of the electrode, and the metabolic potential of the community members, resulting in catalytic flexibility of BESs in converting between different forms of energy.<sup>1–3</sup> To date, electroactive biofilms are most commonly applied in microbial fuel cells (MFCs),<sup>4–6</sup> which convert chemical energy into electrical energy (electrogenesis) by donating electrons liberated from the microbial oxidation of organics to an anode (an electrode operated at a relatively oxidizing potential), and microbial electrosynthesis systems (MESs), which convert electrical energy into chemical energy (electrotrophy) using electrons donated from a cathode (an electrode operated at a relatively reducing potential) for microbial fixation of carbon dioxide to organic compounds.<sup>1,7</sup> The vast majority of BES-related studies

have focused on enriching an electroactive microbial community that functions as either a cathode or anode catalyst, although temporary bidirectional currents were observed in systems that utilize polarity reversal to overcome pH limitations.<sup>8–10</sup> In other studies, a mature biofilm was grown on an anode before switching to cathodic operation permanently to test electrotrophic properties of traditionally anodic organisms.<sup>11–13</sup> Recently, a MES and MFC were hydraulically coupled into a microbial rechargeable battery,<sup>14</sup> although each functionality was maintained on separate electrodes.

To date, enduring bifunctional microbial bioelectrodes have been observed only in phototrophic systems, where anodic current results from consumption of photosynthetic end products (oxygen and fixed carbon).<sup>15–17</sup> In these systems, reduction of oxygen produced by phototrophic microorganisms during carbon fixation, which occurs only during illumination, generated cathodic currents. In the dark, anodic currents were observed because of the microbial oxidation of fixed carbon after oxygen depletion. Accordingly, significant anodic currents were produced only in the dark and cathodic currents only in

**Received:** August 9, 2017

**Accepted:** August 23, 2017

**Published:** August 23, 2017

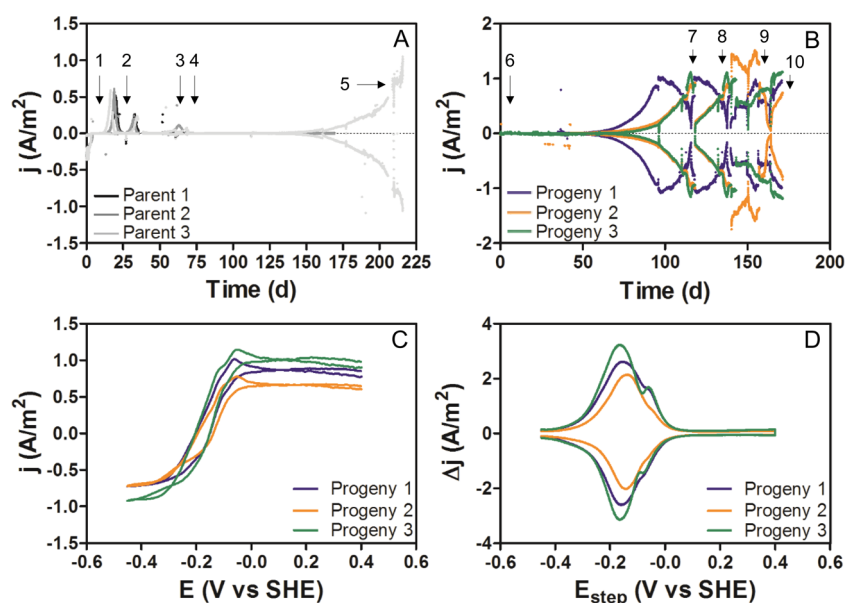


**Figure 1.** (A) Development of the nonphotosynthetic bifunctional electrode in parent reactors. Numbers on the graph correspond to (1) inoculation and addition of 5 mM acetate, (2) addition of 1 mM acetate, (3) the first indication of bidirectional current, (4) parents 1 and 2 killed, and (5) maximum bifunctional current density production by parent 3. (B) Development of the bifunctional electrode in the progeny reactors. Numbers on the graph correspond to (6) inoculation from parent 3, (7) medium replacement, (8) medium replacement and electrode sampling from progeny 3 for confocal microscopy, (9) electrode sampling from progeny 1 and 2 for confocal microscopy, and (10) CV and SWV depicted in panels C and D. (C) Voltammograms of triplicate reactors taken at the end of the experiment (point 10 in panel B) exhibiting bifunctionality on the anodic and cathodic limits of the scan. (D) Square wave voltammograms exhibiting two reversible redox peaks at  $-0.15$  and  $-0.05$  V, although the peak at  $-0.15$  V is clearly dominant.

the light.<sup>16</sup> Additionally, these photosynthetic systems were limited by relatively low current densities ( $0.01$ – $0.08$  A/m<sup>2</sup>).

Here, we demonstrate enrichment of a nonphotosynthetic electroactive biofilm capable of alternating between power generation and energy storage on a single electrode by repeatedly switching the electrode potential between  $-0.4$  V<sub>SHE</sub> where it acts a cathode, and  $0.0$  V<sub>SHE</sub> where it acts as an anode. The current densities in each mode observed here ( $\pm 1.4 \pm 0.4$  A/m<sup>2</sup>) are comparable to what is observed for microbial biocathodic<sup>18,19</sup> and bioanodic<sup>20,21</sup> systems using cloth or planar electrodes, and an order of magnitude higher than those of photosynthetic bifunctional electrodes.<sup>16</sup> These results indicate the feasibility of producing a self-sustaining BES biofilm capable of energy conversion and storage.

## MATERIALS AND METHODS

**Reactor Setup.** Two-chambered reactors (triplicate) were set up as previously described,<sup>12</sup> except that a cation exchange membrane (CMI-7000, Membranes International) was used. The volume of each chamber was 180 mL (120 mL of medium, 60 mL of headspace). The working electrode was fabricated by attaching a titanium wire to a piece of HCl-treated carbon cloth (5 cm × 5 cm) with a titanium nut and bolt. The counter electrode was platinum mesh attached to a titanium wire, and the reference electrode was Ag/AgCl [3 M NaCl; +210 mV vs the standard hydrogen electrode (SHE)]. All potentials reported here are in reference to the SHE. The reactors were stirred at 150 rpm, not temperature controlled, and covered to exclude light.

The reactors were autoclaved and then filled with anaerobic artificial seawater medium (ASW), prepared as previously described,<sup>22</sup> except the medium was sparged with an 80%/20% N<sub>2</sub>/CO<sub>2</sub> mix for 25 min to remove oxygen. Reactors were filled

in an anaerobic glovebox (COY Laboratories) and then flushed with an 80%/20% N<sub>2</sub>/CO<sub>2</sub> gas mix. The initial pH was 6.3.

**Reactor Inoculation and Operation.** Electrochemical characterization of the working electrodes was performed by cyclic voltammetry (CV) and square wave voltammetry (SWV) before and after each medium exchange using a multichannel potentiostat (VMP3, BioLogic). Potentials were scanned between  $-0.45$  and  $0.6$  V<sub>SHE</sub> at 1 mV/s during CV. SWV was conducted over the same potential range with a 25 mV pulse height, a 250 ms pulse width, and a 0.5 mV step size.

After background electrochemical characterization, an inoculum was obtained from the anode of a sediment-based BES operated for  $\sim 2$  years with a power supply stepped between 0.3 and 0.9 V (cell voltage) every 6 h (see the Supporting Information for details). Fibers from the sediment bottlebrush electrode were removed and placed into three tubes containing ASW. The tubes were sonicated, and 20 mL was inoculated into triplicate reactors. Acetate was added to the inoculum (5 mM) and during the first medium exchange (1 mM) to stimulate electroactive microorganisms but was not used in any subsequent exchanges or progeny reactors. The potentials of the working electrodes were stepped between 0.0 and  $-0.4$  V for 10 min each, and current data were collected over time. The potential used during cathodic operation here ( $-0.4$  V) is considerably more positive than that often used for acetate production in MESs ( $-0.6$  to  $-1$  V<sup>7,18,23,24</sup>) reliant on electrode-generated H<sub>2</sub> as an electron transfer mediator, but lower than the potential (0.3 V) used for aerobic electroautotrophic cathodic enrichments not dependent on H<sub>2</sub>.<sup>22,25,26</sup> Killed controls were achieved by exchanging the medium of one reactor with oxygen-saturated medium and by removing the reference electrode lead from another reactor during operation, inducing a large current in the working electrode. To

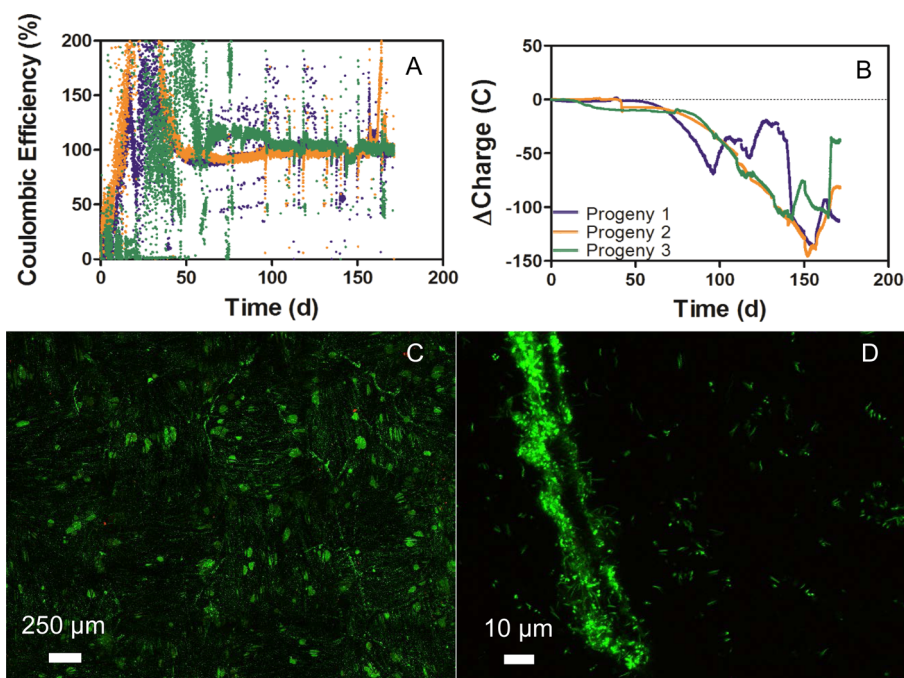


**Figure 2.** (A) Coulombic efficiency of each cycle over the duration of the experiment. A cycle is defined as each 20 min period consisting of 10 min poised at a cathodic potential ( $-0.4$  V) followed by 10 min poised at an anodic potential ( $0.0$  V). Here, each point represents the ratio of the charge produced as an anode to the charge consumed as a cathode during each 20 min period. It should be noted that significant current was not produced until approximately day 50. Accordingly, CE data obtained prior to day 50 are difficult to interpret. After day 50, the bulk of the noise occurs when the medium was exchanged in the reactors. (B) Net change in charge over the duration of the experiment. Charge consumed as a cathode was subtracted from the charge produced as an anode resulting in a net imbalance of charge skewed toward the cathodic reaction (depicted as negative here). We should note that the overall net change in charge is small compared to the total charge passed through the system over the duration of the experiment ( $6250 \pm 750$  C as an anode and  $6300 \pm 800$  C as a cathode). (C and D) Confocal laser scanning microscope images of the biofilm on the electrode surface treated with Live/Dead stain taken with  $10\times$  and  $60\times$  objectives, respectively. The green fluorescence indicates an intact cell membrane.

assess the reproducibility and transferability of the system, three progeny reactors were inoculated with 10 mL of solution immediately surrounding the working electrode of the viable parent reactor after the maximum current was achieved. Medium exchanges took place periodically in a glovebox. The reactor headspace was not continuously flushed.

**Calculations.** Chronoamperometry data exhibited an initial transient current spike immediately after each potential change followed by a relatively steady current output for the remainder of the 10 min period. The current spike (observed in all reactors) is attributed to capacitance charging (exponential current decay with time,  $\sim 0.3$  s) and is excluded from the data analysis. The steady state current was separated and averaged using an Excel-based macro to enable better visualization of the system performance.

Coulombic efficiency, defined as the ratio of charge produced at the electrode during anodic operation to the charge consumed at the electrode during cathodic operation, was calculated by integrating the steady state current over time for each cycle. We should note the possibility that some charge transfer may be masked by the capacitive transient current spikes, and its exclusion is a potential source of error in our Coulombic efficiency.

**Chemical Analysis.** The headspace gas composition was regularly monitored by injecting a  $250 \mu\text{L}$  sample into a gas chromatograph (Peak Laboratories) equipped with TCD (hydrogen and methane detection) and RCP (hydrogen and carbon monoxide detection) detectors. Ultra-high-purity ( $>99.999\%$ ) nitrogen was used as the carrier gas.

Before the reactor medium was exchanged, a sample was taken, filtered into sterile tubes, and stored at  $-20$  °C for further analysis. Samples were then thawed, and  $25 \mu\text{L}$  was injected into a high-performance liquid chromatograph (Agilent) equipped with a diode array detector to detect and quantify volatile fatty acids.

**Microscopy.** The biofilm coverage of the electrode was qualitatively assessed using confocal laser scanning microscopy using similar methods as previously described.<sup>19</sup> Pieces ( $1 \text{ cm} \times 1 \text{ cm}$ ) of the carbon cloth electrode were removed using a sterile razor blade and tweezers in an anaerobic chamber, stained with LIVE/DEAD BaLight stain (ThermoFisher) diluted in  $1\times$  phosphate-buffered saline, gently washed by serial medium exchange, and mounted in a chambered cover slide. At least five sections of each surface were imaged using a Nikon A1RSi confocal microscope.

## RESULTS AND DISCUSSION

**Development of a Nonphotosynthetic Bifunctional Electroactive Biofilm.** A bifunctional electroactive biofilm was developed on a carbon cloth electrode by repeatedly switching the electrode potential between  $-0.4$  and  $0.0$   $V_{\text{SHE}}$  every 10 min (Figure 1A). Alternating anodic and cathodic currents that increased in lock step began 150 days after inoculation. Zero and 20 days after inoculation, 5 and 1 mM acetate was added to three replicate reactors (ASW medium) as a carbon and electron source to stimulate biofilm growth, resulting in unsustained anodic current (peaks labeled 1 and 2). At approximately 45 days, the onset of anodic and cathodic

currents above background [abiotic control (Figure S1)] occurred without additional acetate (labeled 3), providing the first evidence of bifunctionality. During a medium exchange at 60 days (fresh ASW medium, no acetate), two of the reactors were sacrificed for killed controls (see Materials and Methods). Current production ceased, indicating that the observed bidirectional currents were likely due to biological activity. The remaining operational reactor [parent 3 (Figure 1A)] began to produce significant alternating anodic and cathodic current 20 days after the medium exchange, and an exponential increase in current began after 50 days (150 days total after inoculation). The long lag time is consistent with the involvement of slow-growing autotrophic microorganisms, which would contribute to the cathodic current (energy storage) if electrons supplied by the electrode were used to fix carbon dioxide to organic compounds,<sup>19</sup> enabling subsequent anodic current (electricity generation) if electrons passed to the electrode resulted from the oxidation of the same organic compounds. These results demonstrate for the first time an electroactive biofilm that is adept at using an electrode as an electron donor and acceptor.

To verify that the bifunctional biofilm enrichment was reproducible and transferrable, three new reactors containing carbon cloth electrodes were inoculated from the parent 3 bifunctional electrode after it had reached a maximum current density of  $\pm 1$  A/m<sup>2</sup>. Alternating anodic and cathodic currents developed in all three progeny reactors in much less time than in the parent reactor ( $\sim 50$  days, no acetate), consistent with enrichment, to a maximum of  $\pm 1.4 \pm 0.4$  A/m<sup>2</sup>. Currents began to decrease after 100 days, possibly because of pH inhibition (pH 3.0), but recovered after medium exchange (Figure 1B). Current densities from the bifunctional electrode are on the same order of magnitude as those previously observed in other microbial biocathodes<sup>18,19</sup> and bioanodes<sup>20,21</sup> using cloth or planar electrodes.

**Electrochemical Characteristics.** Cyclic voltammograms (Figure 1C) exhibited a single sigmoidal curve centered at  $-0.15$  V<sub>SHE</sub> with stable anodic and cathodic limiting current densities equal to those observed during chronoamperometry.<sup>27,28</sup> Such bifunctionality in a single CV has not been previously observed for an electroactive biofilm and suggests that the same redox cofactor(s) or redox cofactors with similar formal potentials mediate heterogeneous electron transfer across the biofilm–electrode interface when the electrode is operated as an anode and a cathode. The electrode also exhibited major reversible redox peaks at  $-0.15$  V<sub>SHE</sub> and shoulder peaks at  $-0.05$  V<sub>SHE</sub>, indicated by SWV (Figure 1D), close to the midpoint potentials of distinct putative electron transport pathways of *Geobacter sulfurreducens*,<sup>29</sup> a potential member of the enriched biofilm due to the source of its original inoculum (marine sediment). All replicates had redox peaks with similar peak potentials and magnitudes, suggesting a functionally similar community in each reactor.

The stable current density produced by the bifunctional enrichments during anodic operation closely mirrored the stable current density consumed during cathodic operation throughout the experiment, yielding an overall Coulombic efficiency (CE) of  $98 \pm 0.4\%$  based on the ratio of anodic to cathodic charge per charge–discharge cycle (Figure 2A). As current density increased over time, the cathodic charge produced slightly outpaced the anodic charge (Figure 2B), indicating an imbalance in the processes occurring in the system. However, the total charge returned toward zero

(generated minus consumed) when the current density decreased, which suggests that product formation outpaced consumption, resulting in accumulation. Alternatively, the imbalance may be due to formation of multiple products, with some that are consumed more readily by putative electrogenic microorganisms. These results suggest that a single BES community can be used to interconvert between energy storage and power generation at rates comparable to those achieved by electroactive biofilms able to catalyze only one process or the other.

**Energy Storage Compounds.** On the basis of chronoamperometry (Figure 1A,B) and cyclic voltammetry (Figure 1C), we hypothesize that the anodic current is enabled by microbial oxidation of energy-rich compounds generated by cathodic reactions. The reactor headspace and medium were analyzed in an attempt to identify typical MES metabolites and gain insights into potential processes occurring. Hydrogen and carbon monoxide were detected in reactor headspaces throughout the experiment (Figure S2) using gas chromatography. Methane was detected in all parent reactors, but only transiently in one progeny reactor. The steady concentration of hydrogen and carbon monoxide was significantly lower in the headspace of the progeny reactors [ $\sim 10$  ppm of H<sub>2</sub> and  $\sim 0.5$  ppm of CO (Figure S2)] than in the parent reactors [ $\sim 50$  ppm of H<sub>2</sub> and  $\sim 4$  ppm of CO (Figure S2)] and the abiotic control [ $\sim 100$  ppm of H<sub>2</sub> and  $\sim 15$  ppm of CO (Figure S2)], suggesting that these compounds were charge carriers in the system. Hydrogen is a known charge carrier in MESs<sup>30</sup> whose formation is enhanced by cells and enzymes.<sup>31–34</sup> We also consistently detected CO, an electron donor and/or carbon source for many anaerobic metabolic processes,<sup>35,36</sup> including electrogenesis,<sup>37</sup> suggesting it is a charge carrier in this system. While hydrogen and CO can serve as mediators for synthesis of organic compounds, some microorganisms<sup>19,25</sup> and extracellular enzymes<sup>12,31,38–40</sup> can directly accept electrons from solid electron donors for H<sub>2</sub> or CO formation. Carbon monoxide can also be produced as a byproduct of incomplete microbial oxidation of organic compounds.<sup>41</sup> No volatile fatty acids (formate, acetate, propionate, or butyrate) were detected in the progeny reactors, as evidenced by high-performance liquid chromatography (HPLC) analysis. This may indicate the production of a compound that cannot be detected using these HPLC conditions. Alternatively, the efficient utilization of the compound(s) produced by the microbial community over the short cycle duration may have prevented accumulation of the product in the reactor. Although we were unable to detect reduced carbon compounds in the reactor, the system could theoretically support  $\sim 10^8$  acetogens (see the Supporting Information for calculations),<sup>42,43</sup> a plausible CO<sub>2</sub>-fixation process occurring under these conditions. The lag in bidirectional current production supports the notion that electrogenesis is dependent on reduced carbon produced by slow-growing autotrophic organisms. The high CE, sigmoidal CV that spans anodic and cathodic limiting currents, and lock step increase in anodic and cathodic currents may also indicate a prominent role of surface-bound redox enzymes as anodic and cathodic catalysts, as previously described.<sup>12,31,32,40</sup> Charge storage in biofilms may also occur,<sup>44,45</sup> but this alone cannot explain the observed biofilm growth, which requires CO<sub>2</sub> fixation. Follow-up experiments are necessary to identify direct electron transport mechanisms and other potential charge carriers in addition to the ones suggested here.

**Microscopy.** Cells were observed across the surface of the electrodes analyzed by confocal laser scanning microscopy (Figure 2). A majority of cell membranes were intact, indicated by the Live/Dead stained samples, and cells were present as small clusters and single cells with larger clusters interspersed across the electrode surface. The extent of cellular coverage of the electrode surface is significantly lower than what is observed in typical anodic biofilms but is similar to those of previously imaged electroautotrophic biofilms.<sup>19</sup> The relatively sparse surface coverage suggests that improvements to the system can be made to increase performance.

The results presented here support the notion that biological activity is responsible for the bidirectional current. At this time, the organism(s) responsible, the biomolecular machinery, and additional electron storage compounds have yet to be identified. Mechanisms underpinning the production of energetic compounds have not been elucidated as no correlation could be made between the electrochemical performance and the presence of any of the compounds assayed. It is also unknown if a single microorganism is responsible for bidirectional currents or if multiple microorganisms or extracellular enzymes<sup>31</sup> are involved. A community analysis and comparative transcriptional analysis are currently underway, which may yield additional insights.

## ■ ASSOCIATED CONTENT

### ● Supporting Information

The Supporting Information is available free of charge on the ACS Publications website at DOI: [10.1021/acs.estlett.7b00335](https://doi.org/10.1021/acs.estlett.7b00335).

Source of the inoculum, headspace gas concentrations, and plausibility of acetogenesis calculations (PDF)

## ■ AUTHOR INFORMATION

### Corresponding Author

\*E-mail: [matt.yates@nrl.navy.mil](mailto:matt.yates@nrl.navy.mil). Phone: 202-404-6034.

### ORCID

Matthew D. Yates: 0000-0003-4373-3864

### Present Address

<sup>||</sup>J.S.: Economics Department, Dickinson College, Carlisle, PA 17014.

### Notes

The authors declare no competing financial interest.

## ■ ACKNOWLEDGMENTS

Funding provided by the Naval Research Laboratory. The authors thank Qioaping Zhang at the U.S. Salinity Laboratory for assisting with HPLC analysis.

## ■ REFERENCES

- (1) Rabaey, K.; Rozendal, R. A. Microbial electrosynthesis—revisiting the electrical route for microbial production. *Nat. Rev. Microbiol.* **2010**, *8*, 706–716.
- (2) Logan, B. E.; Rabaey, K. Conversion of wastes into bioelectricity and chemicals by using microbial electrochemical technologies. *Science* **2012**, *337*, 686–690.
- (3) Logan, B. E. Exoelectrogenic bacteria that power microbial fuel cells. *Nat. Rev. Microbiol.* **2009**, *7*, 375–381.
- (4) Logan, B. E. *Microbial fuel cells*; John Wiley & Sons, Inc.: Hoboken, NJ, 2008; p 300.
- (5) Logan, B. E.; Aelterman, P.; Hamelers, B.; Rozendal, R.; Schröder, U.; Keller, J.; Freguia, S.; Verstraete, W.; Rabaey, K.

Microbial fuel cells: Methodology and technology. *Environ. Sci. Technol.* **2006**, *40*, 5181–5192.

(6) Harnisch, F.; Schroder, U. From MFC to MXC: chemical and biological cathodes and their potential for microbial bioelectrochemical systems. *Chem. Soc. Rev.* **2010**, *39*, 4433–4448.

(7) Marshall, C. W.; Ross, D. E.; Fichot, E. B.; Norman, R. S.; May, H. D. Electrosynthesis of commodity chemicals by an autotrophic microbial community. *Appl. Environ. Microbiol.* **2012**, *78*, 8412–20.

(8) Cheng, K. Y.; Ginige, M. P.; Kaksonen, A. H. Ano-Cathophilic Biofilm Catalyzes Both Anodic Carbon Oxidation and Cathodic Denitrification. *Environ. Sci. Technol.* **2012**, *46*, 10372–10378.

(9) Yang, Y.; Qin, M.; Yang, X.; He, Z. Enhancing hydrogen production in microbial electrolysis cells by in situ hydrogen oxidation for self-buffering pH through periodic polarity reversal. *J. Power Sources* **2017**, *347*, 21–28.

(10) Li, W.; Sun, J.; Hu, Y.; Zhang, Y.; Deng, F.; Chen, J. Simultaneous pH self-neutralization and bioelectricity generation in a dual bioelectrode microbial fuel cell under periodic reversion of polarity. *J. Power Sources* **2014**, *268*, 287–293.

(11) Hartline, R. M.; Call, D. F. Substrate and electrode potential affect electrotrophic activity of inverted bioanodes. *Bioelectrochemistry* **2016**, *110*, 13–18.

(12) Yates, M. D.; Siegert, M.; Logan, B. E. Hydrogen evolution catalyzed by viable and non-viable cells on biocathodes. *Int. J. Hydrogen Energy* **2014**, *39*, 16841–16851.

(13) Yun, H.; Liang, B.; Kong, D. Y.; Cheng, H. Y.; Li, Z. L.; Gu, Y. B.; Yin, H. Q.; Wang, A. J. Polarity inversion of bioanode for biocathodic reduction of aromatic pollutants. *J. Hazard. Mater.* **2017**, *331*, 280–288.

(14) Molenaar, S. D.; Mol, A. R.; Sleutels, T. H. J. A.; ter Heijne, A.; Buisman, C. J. N. Microbial Rechargeable Battery: Energy Storage and Recovery through Acetate. *Environ. Sci. Technol. Lett.* **2016**, *3*, 144–149.

(15) Strik, D. P. B. T. B.; Hamelers, H. V. M.; Buisman, C. J. N. Solar Energy Powered Microbial Fuel Cell with a Reversible Bioelectrode. *Environ. Sci. Technol.* **2010**, *44*, 532–537.

(16) Darus, L.; Lu, Y.; Ledezma, P.; Keller, J.; Freguia, S. Fully reversible current driven by a dual marine photosynthetic microbial community. *Bioresour. Technol.* **2015**, *195*, 248–253.

(17) Malik, S.; Drott, E.; Grisdela, P.; Lee, J.; Lee, C.; Lowy, D. A.; Gray, S.; Tender, L. M. A self-assembling self-repairing microbial photoelectrochemical solar cell. *Energy Environ. Sci.* **2009**, *2*, 292–298.

(18) Marshall, C. W.; Ross, D. E.; Fichot, E. B.; Norman, R. S.; May, H. D. Long-term Operation of Microbial Electrosynthesis Systems Improves Acetate Production by Autotrophic Microbiomes. *Environ. Sci. Technol.* **2013**, *47*, 6023–6029.

(19) Yates, M. D.; Eddie, B. J.; Kotloski, N. J.; Lebedev, N.; Malanoski, A. P.; Lin, B.; Strycharz-Glaven, S. M.; Tender, L. M. Toward understanding long-distance extracellular electron transport in an electroautotrophic microbial community. *Energy Environ. Sci.* **2016**, *9*, 3544–3558.

(20) Zhang, X.; Philips, J.; Roume, H.; Guo, K.; Rabaey, K.; PrévotEAU, A. Rapid and Quantitative Assessment of Redox Conduction Across Electroactive Biofilms by using Double Potential Step Chronoamperometry. *ChemElectroChem* **2017**, *4*, 1026–1036.

(21) Flexer, V.; Marque, M.; Donose, B. C.; Viridis, B.; Keller, J. Plasma treatment of electrodes significantly enhances the development of anodic electrochemically active biofilms. *Electrochim. Acta* **2013**, *108*, 566–574.

(22) Wang, Z.; Leary, D. H.; Malanoski, A. P.; Li, R. W.; Hervey, W. J.; Eddie, B. J.; Tender, G. S.; Yanosky, S. G.; Vora, G. J.; Tender, L. M.; Lin, B.; Strycharz-Glaven, S. M. A previously uncharacterized, nonphotosynthetic member of the *Chromatiaceae* is the primary CO<sub>2</sub>-fixing constituent in a self-regenerating biocathode. *Appl. Environ. Microbiol.* **2015**, *81*, 699–712.

(23) Jourdin, L.; Freguia, S.; Donose, B. C.; Chen, J.; Wallace, G. G.; Keller, J.; Flexer, V. A novel carbon nanotube modified scaffold as an efficient biocathode material for improved microbial electrosynthesis. *J. Mater. Chem. A* **2014**, *2*, 13093–13102.

- (24) Jourdin, L.; Grieger, T.; Monetti, J.; Flexer, V.; Freguia, S.; Lu, Y.; Chen, J.; Romano, M.; Wallace, G. G.; Keller, J. High Acetic Acid Production Rate Obtained by Microbial Electrosynthesis from Carbon Dioxide. *Environ. Sci. Technol.* **2015**, *49*, 13566–74.
- (25) Eddie, B. J.; Wang, Z.; Hervey, W. J.; Leary, D. H.; Malanoski, A. P.; Tender, L. M.; Lin, B.; Strycharz-Glaven, S. M. Metatranscriptomics Supports the Mechanism for Biocathode Electroautotrophy by “*Candidatus Tenderia electrophaga*”. *mSystems* **2017**, *2*, e00002-17.
- (26) Desmond-Le Quémener, E.; Rimboud, M.; Bridier, A.; Madigou, C.; Erable, B.; Bergel, A.; Bouchez, T. Biocathodes reducing oxygen at high potential select biofilms dominated by Ectothiorhodospiraceae populations harboring a specific association of genes. *Bioresour. Technol.* **2016**, *214*, 55–62.
- (27) Snider, R. M.; Strycharz-Glaven, S. M.; Tsoi, S. D.; Erickson, J. S.; Tender, L. M. Long-range electron transport in *Geobacter sulfurreducens* biofilms is redox gradient-driven. *Proc. Natl. Acad. Sci. U. S. A.* **2012**, *109*, 15467–15472.
- (28) Liu, Y.; Kim, H.; Franklin, R. R.; Bond, D. R. Linking Spectral and Electrochemical Analysis to Monitor *c*-type Cytochrome Redox Status in Living *Geobacter sulfurreducens* Biofilms. *ChemPhysChem* **2011**, *12*, 2235–2241.
- (29) Yoho, R. A.; Popat, S. C.; Torres, C. I. Dynamic Potential-Dependent Electron Transport Pathway Shifts in Anode Biofilms of *Geobacter sulfurreducens*. *ChemSusChem* **2014**, *7*, 3413–3419.
- (30) Jourdin, L.; Lu, Y.; Flexer, V.; Keller, J.; Freguia, S. Biologically Induced Hydrogen Production Drives High Rate/High Efficiency Microbial Electrosynthesis of Acetate from Carbon Dioxide. *ChemElectroChem* **2016**, *3*, 581–591.
- (31) Deutzmann, J. S.; Sahin, M.; Spormann, A. M. Extracellular Enzymes Facilitate Electron Uptake in Biocorrosion and Bioelectrosynthesis. *mBio* **2015**, *6*, e00496-15.
- (32) Deutzmann, J. S.; Spormann, A. M. Enhanced microbial electrosynthesis by using defined co-cultures. *ISME J.* **2017**, *11*, 704.
- (33) Aulenta, F.; Catapano, L.; Snip, L.; Villano, M.; Majone, M. Linking bacterial metabolism to graphite cathodes: Electrochemical insights into the H<sub>2</sub>-producing capability of *Desulfovibrio sp.* *ChemSusChem* **2012**, *5*, 1080–1085.
- (34) Geelhoed, J. S.; Stams, A. J. M. Electricity-assisted biological hydrogen production from acetate by *Geobacter sulfurreducens*. *Environ. Sci. Technol.* **2011**, *45*, 815–820.
- (35) Oelgeschläger, E.; Rother, M. Carbon monoxide-dependent energy metabolism in anaerobic bacteria and archaea. *Arch. Microbiol.* **2008**, *190*, 257–269.
- (36) Mörsdorf, G.; Frunzke, K.; Gadkari, D.; Meyer, O. Microbial growth on carbon monoxide. *Biodegradation* **1992**, *3*, 61–82.
- (37) Mehta, P.; Hussain, A.; Tartakovsky, B.; Neburchilov, V.; Raghavan, V.; Wang, H.; Guiot, S. R. Electricity generation from carbon monoxide in a single chamber microbial fuel cell. *Enzyme Microb. Technol.* **2010**, *46*, 450–455.
- (38) Reda, T.; Plugge, C. M.; Abram, N. J.; Hirst, J. Reversible interconversion of carbon dioxide and formate by an electroactive enzyme. *Proc. Natl. Acad. Sci. U. S. A.* **2008**, *105*, 10654–10658.
- (39) Armstrong, F. A.; Belsey, N. A.; Cracknell, J. A.; Goldet, G.; Parkin, A.; Reisner, E.; Vincent, K. A.; Wait, A. F. Dynamic electrochemical investigations of hydrogen oxidation and production by enzymes and implications for future technology. *Chem. Soc. Rev.* **2009**, *38*, 36–51.
- (40) Armstrong, F. A.; Hirst, J. Reversibility and efficiency in electrocatalytic energy conversion and lessons from enzymes. *Proc. Natl. Acad. Sci. U. S. A.* **2011**, *108*, 14049–14054.
- (41) Lupton, F. S.; Conrad, R.; Zeikus, J. G. CO metabolism of *Desulfovibrio vulgaris* strain Madison: physiological function in the absence or presence of exogeneous substrates. *FEMS Microbiol. Lett.* **1984**, *23*, 263–268.
- (42) Daniel, S. L.; Hsu, T.; Dean, S. I.; Drake, H. L. Characterization of the H<sub>2</sub>- and CO-dependent chemolithotrophic potentials of the acetogens *Clostridium thermoaceticum* and *Acetogenium kivui*. *J. Bacteriol.* **1990**, *172*, 4464–4471.
- (43) Phillips, R.; Milo, R. A feeling for the numbers in biology. *Proc. Natl. Acad. Sci. U. S. A.* **2009**, *106*, 21465–21471.
- (44) Bonanni, P. S.; Schrott, G. D.; Robuschi, L.; Busalmen, J. P. Charge accumulation and electron transfer kinetics in *Geobacter sulfurreducens* biofilms. *Energy Environ. Sci.* **2012**, *5*, 6188–6195.
- (45) Deeke, A.; Sleutels, T. H. J. A.; Hamelers, H. V. M.; Buisman, C. J. N. Capacitive Bioanodes Enable Renewable Energy Storage in Microbial Fuel Cells. *Environ. Sci. Technol.* **2012**, *46*, 3554–3560.